Force-serial and Force-parallel Actuation Placement for Topology Optimization of Adaptive Structures

Gennaro Senatore[*]

*Institute for Lightweight Structures and Conceptual Design (ILEK), University of Stuttgart
gennaro.senatore@ilek.uni-stuttgart.de

Abstract

Topology optimization for adaptive structures involves the synthesis of the structural layout in combination with actuator placement. A recently developed formulation based on mixed-integer programming (MIP) has shown that adaptive solutions approach the limit of material economy (e.g., Michell trusses) and, in parallel, satisfy important constraints including displacements and stability that would not be possible without adaptation. In previous work, the actuators are assumed to be in series with the housing element and therefore subjected to the same force, i.e. force-serial. While this strategy produces very efficient configurations that vastly outperform equivalent topology-optimized passive structures, different solutions could be obtained by considering actuators working in parallel with the housing element, i.e. force-parallel. A force-parallel actuator can take a share of the force carried by the housing element to satisfy equilibrium, compatibility, and stress limits, thus effectively changing the internal force flow. Although the effect of a force-parallel actuator is more local to the housing element compared to a force-serial one concerning displacement compensation, the ability to directly change the stress in highly loaded elements can help satisfy buckling and other stability constraints more efficiently. This work offers a new topology optimization formulation for adaptive structures that considers the placement of force-parallel actuators to investigate the difference with solutions obtained using force-serial actuators.

Keywords: structure-control optimization, topology optimization, adaptive structures, active structural control, ultralightweight design, conceptual design, morphology

1. Introduction

1.1. Previous work

Optimal integration of sensing and actuation systems in civil structures enables significant performance improvement and new functionalities such as continuous monitoring and mitigation of the structural response under loading. Initial investigation into active structural control has focused on vibration suppression for buildings and bridges under extreme events showing significant performance improvement compared to alternative passive isolation systems [1], [2], [3]. Recent investigations have adopted a holistic approach including aspects of lightweight design [4], sustainability [5] as well as reliability [6]. Extensive investigation has shown that the use of active systems is particularly effective for stiffness-governed structures, e.g., tall and slender buildings, long-span floor slabs, and bridges [7]. In these cases, the active compensation of the displacement response is very effective in eliminating overdesign that is typically required to increase the stiffness by adding more material. Quantification of the benefits of this approach has been carried out through numerical and experimental testing. Results have shown that material and overall emissions savings exceed 50% for tall and slender buildings, long-span bridges, and floor slabs [7], [8], [9]. Recent studies provide numerical evidence of the capability

retrofitting active systems that can significantly reduce fatigue-induced damage accumulation in bridge structures [10].

Designing adaptive structures is challenging because it involves the coordination of structural-related features, e.g., element sizing, geometry and topology, and control-related features, e.g., placement of sensor, actuators and determination of control commands. Depending on the formulation specificities, this is typically a nonlinear mixed-integer problem that involves continuous (e.g., element sizing) and binary (e.g., element topology, actuator locations).

A new formulation for integrated structure-control topology optimization is given in [11]. The problem statement is a set of simultaneous equations that include equilibrium, geometric compatibility, and stability. The method is formulated using the Simultaneous Analysis and Design (SAND) approach. Design variables include element topology and sizing and actuator locations. State variables include element forces and deformations, nodal displacements, and control commands. Constraints on stress, displacement and stability are considered as well as control feasibility (e.g., limit on actuator forces). Topology optimization and actuator placement are carried out by minimizing a cost function that includes the structural and actuation system mass. This has enabled an All-In-One (AIO) mixed-integer programming problem formulation that has been solved to a global optimum using deterministic methods, e.g. branch and bound. What sets this new formulation apart from existing methods, is that it can model the interdependencies between design and state variables to evaluate the effect of active control, that is manipulation of the response under loading, on structural topology, element sizing and actuator placement.

1.2. New contribution

In [11], actuators are modeled as in series with the housing elements and therefore are subjected to the same force, i.e. force-serial. While this strategy produces very efficient configurations that vastly outperform equivalent topology-optimized passive structures, different solutions could be obtained by considering actuators working in parallel with the housing element, i.e. force-parallel. A force-parallel actuator can take a share of the force carried by the housing element, thus changing the force flow. Although the effect of a force-parallel actuator is more local to the housing element compared to a force-serial one concerning displacement compensation, the ability to directly change the stress in highly loaded elements can help satisfy buckling and other stability constraints more efficiently.

While force-serial actuators have been investigated in several studies, only a few studies exist that consider force-parallel actuators [12]. A practical implementation of both force-serial and force-parallel actuators has been realized in a 36 m tall adaptive high-rise prototype at the University of Stuttgart [13]. However, no study has yet been carried out that investigates the effect of force-parallel actuation on structural parameters and actuator locations as well as the potential for mass savings. This work offers a new topology optimization formulation for adaptive structures that considers the placement of force-parallel actuators and provides a preliminary evaluation of the difference with solutions obtained using force-serial actuators.

2. Force-serial vs force-parallel actuation

Generally, linear actuators can be installed in series or in parallel with the housing structural element. When in series, the force taken by the actuator is the same as that of the element. Referring to Figure 1a

$$F = F^{el} = F^{act} \tag{1}$$

This assembly can be thought of as that of two springs in series, as illustrated in Figure 1b. Since the springs are in series, the reciprocal of the assembly stiffness is equal to the sum of the reciprocal of the element and actuator stiffness

$$\frac{1}{k} = \frac{1}{k^{el}} + \frac{1}{k^{act}} \tag{2}$$

The actuator stiffness k^{act} is usually significantly greater than the element stiffness k^{el} and therefore for simplicity, the assembly stiffness can be approximated as

$$k = k^{el} = \frac{E\alpha}{L} \tag{3}$$

where α is the element cross-section area, E the Young modulus, and L the element length. The strain of the assembly is equal to the sum of the strains of the two springs. The assembly (element + actuator) constitutive law is

$$\Delta l = e + \Delta L \tag{4}$$

where Δl is the total deformation, e the element elastic deformation caused by F and ΔL the actuator length change.

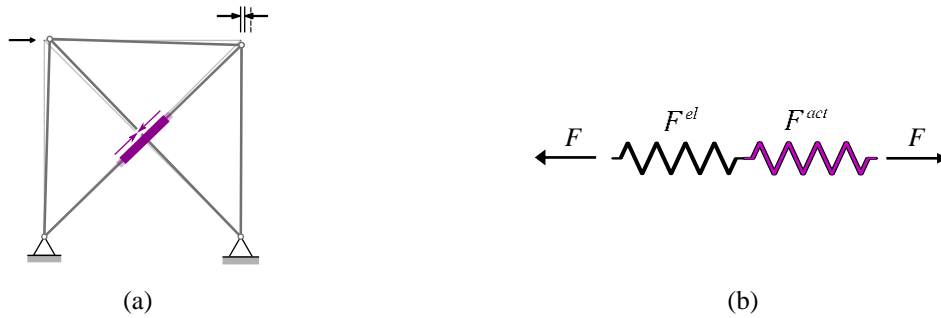(a)   (b)

Figure 1: Force-serial actuation

When the actuator is installed in parallel with the element, which is illustrated in Figure 2, the element and actuator are subjected to the same deformation

$$\Delta l = \Delta L = e \tag{5}$$

The total force in the assembly is the sum of the element and actuator forces

$$F = F^{el} + F^{act} \tag{6}$$

and the same applies to the stiffness

$$k = k^{el} + k^{act} \tag{7}$$

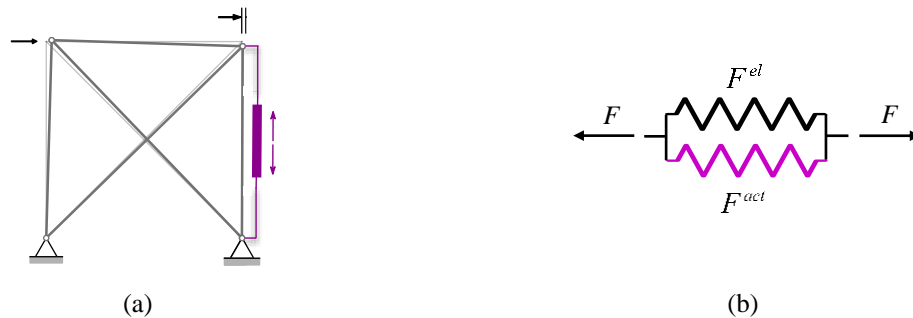

(a)   (b)

Figure 2: Force-parallel actuation

Note that the actuator must connect to the ends of the housing elements to be force-parallel. Otherwise, the actuator force will only affect the element force over length contained between the application points. For long elements, this requires an extension so that the actuator body can be connected to the element ends.

Force-serial actuators can perform significant length changes relative to the strain that limits the housing element. Depending on the quality of the actuator placement, force-serial actuators can efficiently reduce the displacement response, and, for statically indeterminate topologies, have a certain degree of manipulation of the stress response [14]. However, since the actuator must work against the same force the housing element takes, depending on the location, the required force capacity might be high. Force-serial actuation is particularly efficient for stiffness-governed problems, where the ability to reduce displacements outweighs the additional force and mass requirements of the actuators resulting in substantial overall mass reduction compared to equivalent conventional (i.e., passive) configurations.

On the contrary, force-parallel actuators cannot directly manipulate the displacement response, as they are limited by the strain of the housing element. However, the ability to take a share of the force, enables direct manipulation of the housing element deformation and stress, which, depending on the placement quality, can also provide a significant response reduction resulting in material savings. Force-parallel actuators do not work against the main load path (e.g., gravitational load transfer), and therefore can be placed on elements that are subjected to high forces compared to force-serial actuators. The use of semi-active actuators that can modify their stiffness properties could be particularly suitable for force-parallel actuation given their fast response and low energy requirements.

3. All-In-One (AIO) structure-control topology optimization

3.1. Structural topology and actuator assignment

Building on [11], the combined problem of structural topology and actuator placement optimization is formulated through mixed-integer programming (MIP) based on the Ground Structure approach [15]. For brevity, in this work, only equations related to force-parallel actuation are stated, the reader is referred to [11] for the full formulation.

Structural topology and actuator placement optimization are carried out using binary assignment matrices $\mathbf{A}^{el} \in \{0,1\}^{n^{el}}$ and $\mathbf{A}^{act} \in \{0,1\}^{n^{el}}$, respectively, where n^{el} denotes the total number of elements of the Ground Structure (GS). The optimization process consists in obtaining the optimal element set E^{TO} from the initial Ground Structure $E^{TO} \subset E^{GS}$ and simultaneously the actuator optimal location set, which is a subset of the optimized topology $E^{act} \subset E^{TO} \subset E^{GS}$.

$$A_i^{el} = \begin{cases} 1, & \text{if element } i \subset E^{TO} \subset E^{GS} \\ 0, & \text{if element } i \not\subset E^{TO} \subset E^{GS} \end{cases} \tag{8}$$

$$A_i^{act} = \begin{cases} 1, & \text{if actuator } i \subset E^{act} \subset E^{TO} \subset E^{GS} \\ 0, & \text{if actuator } i \not\subset E^{act} \subset E^{TO} \subset E^{GS} \end{cases} \tag{9}$$

3.2. Objective function

The objective function comprises the mass of the structural and actuation systems

$$\min_{\mathbf{X}} \sum_i^{n^{el}} \rho_i a_i L_i + c^{act} \sum_i^{n^{el}} F_i^{actMax} \tag{10}$$

where ρ_i, a_i, and L_i are the material density, cross-section area and length of the ith element, respectively. The element cross-section areas are semi-continuous variables $\boldsymbol{\alpha} \in \mathbb{R}^{n^{el}}$ defined in the range $\{0;(\underline{\alpha},\overline{\alpha})\}$.

The mass of the actuation system is quantified through an assumption of linear proportionality with an auxiliary variable that represents the maximum force required for adaptation, which is denoted $\mathbf{F}^{actMax} \in \mathbb{R}^{n^{el}}$. The maximum actuator force can be compressive or tensile depending on the position of the actuator and boundary conditions. To avoid the absolute value in the objective function, which makes

it nonlinear, $\mathbf{F}^{actMax}$ can only take positive values $\mathbb{R}_{\geq 0}^{n^{el}}$. The proportional constant c^{act} (kg/kN) can be set to fit the specificities of the considered actuation technology. Since the maximum actuation force is an optimization variable included in the objective function, minimization will yield configurations with the minimum combined system mass.

3.3. State conditions and response control

The modeling of force-serial actuators requires two state variables, the length change $\Delta\mathbf{L} \in \mathbb{R}^{n^{el}}$ which is added to the geometric compatibility relations, and the force $\mathbf{F}^{act} \in \mathbb{R}^{n^{el}}$ as well as auxiliary variables to constrain the actuator force to be identical to that of the housing element $\mathbf{F}^{el} \in \mathbb{R}^{n^{el}}$. Force-parallel actuators instead, since the force is added to that of the housing element, require only the force variable in the equilibrium conditions

$$\mathbf{B}\left(\mathbf{F}^{el} + \mathbf{F}^{act} \right) = \mathbf{P} + \mathbf{P}^{sws} + \mathbf{P}^{swa} \tag{11}$$

$$\mathbf{B}_i^T \mathbf{d} = e_i, \forall i \in E^{GS} \tag{12}$$

$$F_i^{el} = \frac{E_i e_i}{L_i} a_i, \forall i \in E^{GS} \tag{13}$$

where $\mathbf{B} \in \mathbb{R}^{n^{dof} \times n^{el}}$ contains the element cosine directions (often referred to as equilibrium matrix), $\mathbf{P} \in \mathbb{R}^{n^{dof}}$ is the external load. Note that $\mathbf{F}^{act}$ is different from $\mathbf{F}^{actMax}$. Generally, depending on the number of load cases n^p, the actuator force is a multi-dimensional vector $\mathbf{F}^{act} \in \mathbb{R}^{n^{el} \times n^p}$ while $\mathbf{F}^{actMax} \in \mathbb{R}^{n^{el} \times 1}$ is always a one-dimensional vector since it is the maximum actuator force required for response control across n^p load cases. The self-weight loads of structure and actuation systems are denoted with $\mathbf{P}^{sws} \in \mathbb{R}^{n^{dof}}$ and $\mathbf{P}^{swa} \in \mathbb{R}^{n^{dof}}$, respectively. Both $\mathbf{P}^{sws}$ and $\mathbf{P}^{swa}$ are variables because they are functions of the element cross-section areas and topology as well as actuator force capacity and placement, respectively. Since the actuators are force-parallel, the geometric compatibility equation (12) does not include $\Delta\mathbf{L}$ and the constitutive equation (13) remains unchanged. The element forces $\mathbf{F} \in \mathbb{R}^{n^{el}}$ are constrained within bounds that account for material and stability stress limits [11]. The same applies to the element strain variable $\mathbf{e} \in \mathbb{R}^{n^{el}}$ and nodal displacements $\mathbf{d} \in \mathbb{R}^{n^{dof}}$ that are constrained by appropriate bounds $\left(\underline{\mathbf{e}}, \bar{\mathbf{e}} \right)$ and $\left(\underline{\mathbf{d}}, \bar{\mathbf{d}} \right)$, respectively, as shown in [11].

3.4. Actuator placement

The actuator force variable $\mathbf{F}^{act}$ is related to the actuator placement through $\mathbf{F}^{actMax}$, the assignment matrix $\mathbf{A}^{act}$ and the actuator force capacity $\left[\underline{F}^{act}, \overline{F}^{act} \right]$, which is the greatest force in tension and compression that can be applied by an actuator. To avoid the absolute value in the objective function, Eq (14) relates $\mathbf{F}^{actMax}$ with the product of the actuator force capacity and assignment matrix

$$\begin{aligned} \mathbf{F}^{actMax} &\leq \overline{F}^{act} \mathbf{A}^{act} \\ -\mathbf{F}^{actMax} &\geq \underline{F}^{act} \mathbf{A}^{act} \end{aligned} \tag{14}$$

Since $A_i^{act} = 0$ when no actuator is placed on the ith element, the corresponding actuator force variable is constrained to zero, which is the intended behavior. The actuator force is constrained within the bounds taken by the variable $\mathbf{F}^{actMax}$ through Eq (15)

$$-\mathbf{F}^{actMax} \leq \mathbf{F}^{act} \leq \mathbf{F}^{actMax} \tag{15}$$

The actuator force bounds are also useful to exclude locations of elements subjected to high forces, for example, low-level columns of multi-story buildings. This way, most element subjected to gravitational loads are usually excluded for the housing of actuators due to the high forces they carry.

The actuator placement is related to the element topology via Eq (16) and the total number of actuators is limited to an assigned upper bound $\bar{n}^{act}$. Although there is no explicit minimization of the number of actuators, since the objective function includes the actuation system mass, the optimal solutions typically have a low number of actuators.

$$A_i^{act} \leq A_i^{el}, \; \forall i \in E^{GS} \tag{16}$$

$$\sum_i A_i^{act} \leq \bar{n}^{act}, \; \forall i \in E^{GS} \tag{17}$$

4. Examples

4.1. Inputs

The examples discussed in this section evaluate the effect on the system mass of force-parallel and force-serial actuation. Although reasonable geometric domains and loading conditions have been considered, the examples are kept as simple as possible, and therefore shall not be considered as representative of real-world scenarios, which is beyond the scope of this article. All simulations are carried out considering the following assumptions:

- Small strains and small displacements.
- All structural elements are made of steel S355 and have a circular hollow section. To reduce the optimization complexity the wall thickness is set to 10% of the outer radius.
- The actuator mass is assumed proportional to the force capacity with a constant $c^{act} = 0.2\,\text{kg/kN}$, which is a reasonable assumption for hydraulic actuators using high-strength steel [17].
- The displacement limits are set as the ratio between the main dimension and the constant $c^{SLS} = 500$.

For all the examples discussed in this work, the problem formulation given in Section 3 has been solved to global optimality with the branch-and-bound algorithm implemented in Gurobi v10 [18].

4.2. Ground structure 1x1, slenderness ratio 1/1

The first example considers a 1x1 ground structure (GS) with a slenderness ratio (SR) of 1/1. The structure is pinned at the lower corner nodes and subjected to a lateral point load applied at the upper left corner node, as illustrated in Figure 3a. The ground structure is kept as simple as possible since this example is employed to demonstrate the difference between the effect of force-parallel and force-serial actuation on element sizing. Figure 3b shows the optimized passive solutions while 3c and 3d the adaptive solutions obtained with force-serial and force-parallel actuation, respectively. All solutions are global optima for the considered problem (i.e., 0% Mip-Gap). Optimization metrics are given in Table 1. Note that for simplicity of representation, parallel actuators are represented as in Figure 3d without covering the whole length of the element to connect at its ends.
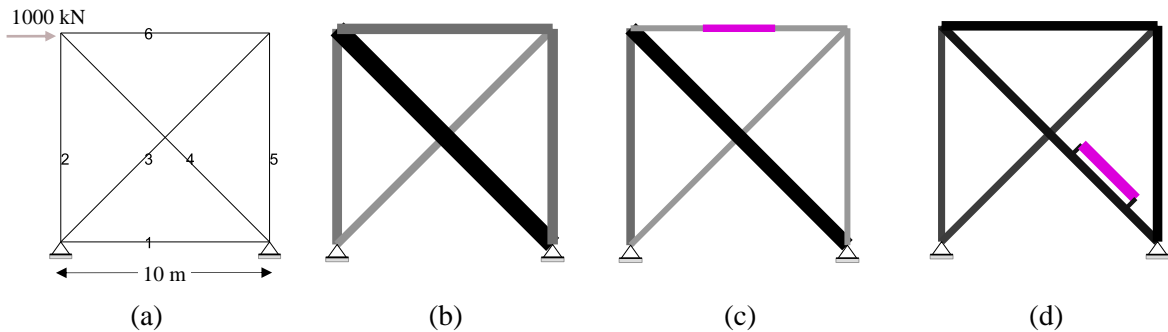

Figure 3 (a) GS 1x1, SR 1/1 (b) passive (c) force-serial (d) force-parallel

Table 1 GS 1x1, SR 1/1: benchmark force-serial vs force-parallel solutions

	m^t (kg)	m^s (kg)	m^{act} (kg)	$\max(\mathbf{r}^e)$ (mm)	n^{act}	$\max(\mathbf{F}^{act})$ (kN)	MIP-Gap	Mass savings
Adaptive force-serial	2048	2034	13.6	141	1	68	0%	6%
Passive	2178	2178	-	141	-	-	0%	
Adaptive force-parallel	1594	1394	200	81	1	1000	0%	27%
Passive	2178	2178	-	141	-	-	0%	

The maximum number of actuators n^{act} is limited to one. Since the force-parallel actuator can take a share of the compression force in element 4, significant stress homogenization is enabled resulting in 27% savings compared to the passive solution. The force-serial solution instead achieves only 6% mass savings.

Figure 4a and b show the controlled stress and displacement response for the force-serial and force-parallel solutions, respectively. The force-serial actuator cannot be placed on element 4 because the force capacity is limited to 1000 kN, while the force in element 4 is greater, as shown in the bar chart of Figure 4c. The force-serial actuator is effective in reducing the displacement caused by the lateral load, however, it has a much smaller effect on the stress response compared to the force-parallel actuator. In this configuration, which is not governed by stiffness (SR of 1/1) the use of force-parallel actuation is more effective to reduce the system mass.
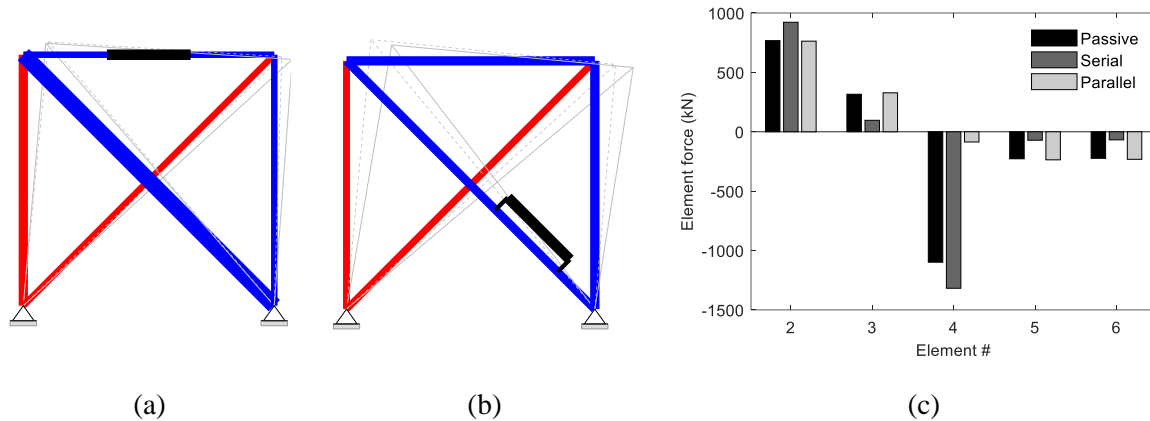

(a)   (b)   (c)

Figure 4 GS 1x1, SR 1/1: stress and displacement response

4.3. Ground structure 4x4, slenderness ratio 1/1

This example considers a ground structure with identical dimensions to the previous example and subdivided in 4x4 cells with a node-neighborhood connectivity (NNC) of 4, which is illustrated in Figure 5a. The loading condition is similar to the previous example. However, symmetry constraints are applied to the element cross-section area and actuator locations to reduce the number of design variables.

Simultaneous force-serial and force-parallel actuator placement is enabled by extending the formulation given in Section 3. An additional binary assignment matrix is defined to enable the choice of force-parallel and force-serial actuators to minimize the system mass. Auxiliary constraints are defined so that only one type of actuator can be placed on an element. For brevity, this formulation extension is not given in this manuscript. The maximum number of actuators is 4.
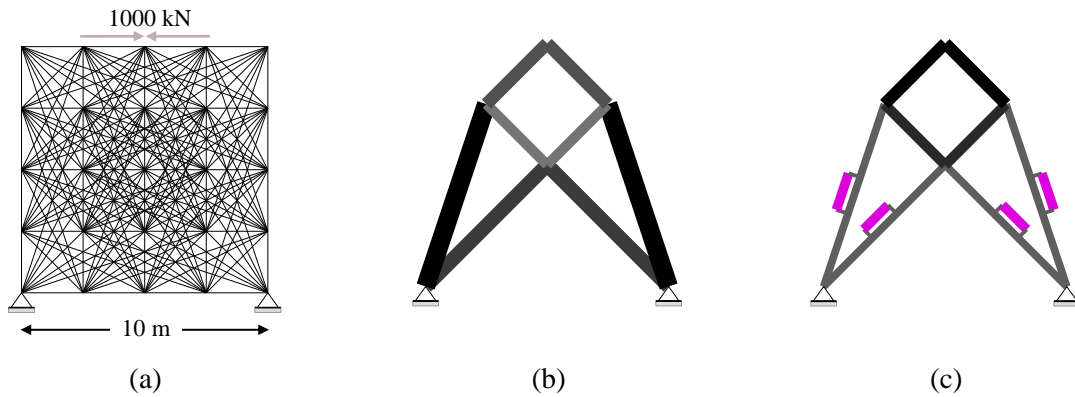
1000 kN

10 m

(a)

(b)

(c)

Figure 5 (a) GS 4x4, SR 1/1 (b) passive (c) adaptive

Figure 5b and c show the passive and adaptive optimal solutions. Since the slenderness ratio is kept at 1/1, the problem is not stiffness-governed. The global optimum is obtained by placing all actuators in parallel to reduce the high forces in the elements that connect directly to the supports. System mass savings of 39% are achieved. A breakdown of the system mass is given in Table 2.

Table 2 GS 4x4, SR 1/1: benchmark passive vs adaptive solution

	m^t (kg)	m^s (kg)	m^{act} (kg)	$\max(\mathbf{r}^e)$ (mm)	n^{act}	$\max(\mathbf{F}^{act})$ (kN)	MIP-Gap	Mass savings
Adaptive	796	447	348	63	4	846	0%	39%
Passive	1310	1310	-	97	-	-	0%	

4.4. Ground structure 4x1, slenderness ratio 5/1

The last example considers a ground structure comprising 4x1 cells, with node-neighborhood connectivity (NNC) of 4 and a slenderness ratio of 5/1. The ground structure and boundary conditions are illustrated in Figure 6a. The maximum number of actuators is set to 4 and the actuator force capacity is limited to 500 kN.

Since the geometric domain has a slenderness ratio significantly higher than that considered in the previous examples, the global optimum for the adaptive solution is obtained by combining force-serial and force-parallel actuators. Figure 6b and c show the passive and adaptive solutions, respectively. Two force-parallel actuators are placed on the second (from the lower side) cell diagonals to reduce the high forces induced by the external load and two force-serial actuators are placed on the fourth cell columns to effectively reduce the top node displacements. The adaptive solution achieves mass savings of 38%. A breakdown of the system mass is given metrics in Table 3.

Table 3 GS 4x1, SR 5/1: benchmark passive vs adaptive solution

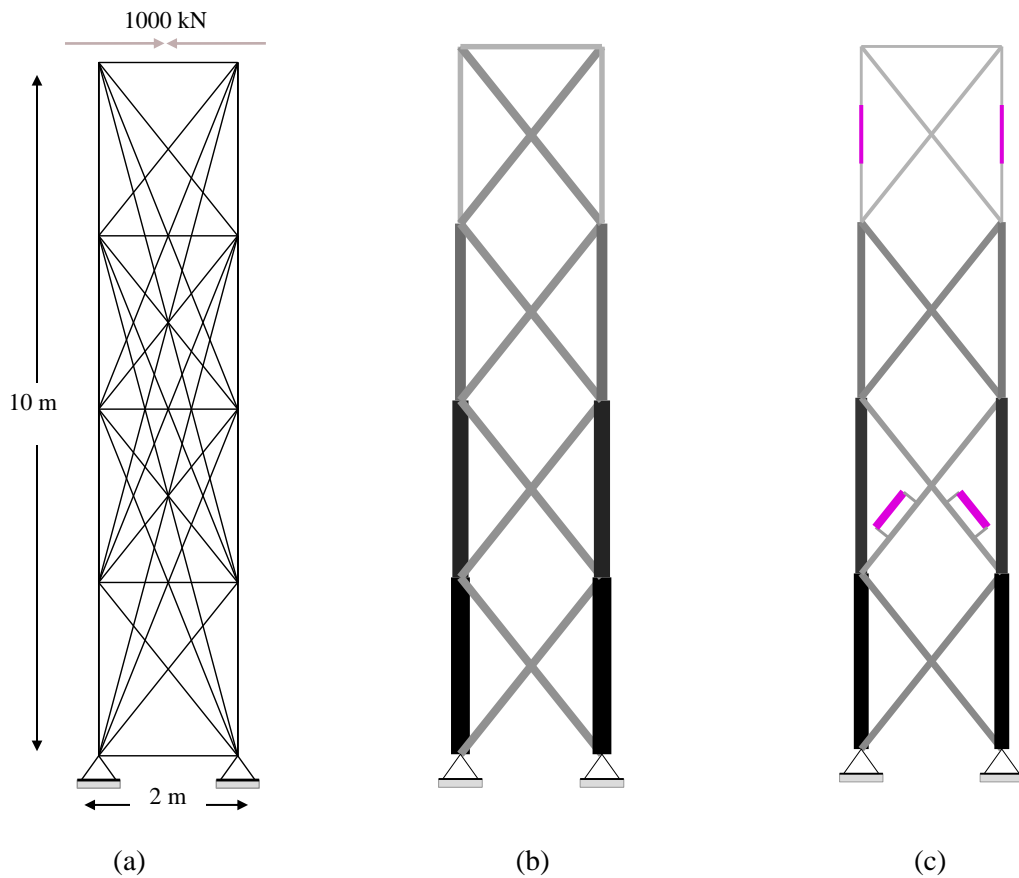|	m^t (kg)	m^s (kg)	m^{act} (kg)	$\max(\mathbf{r}^e)$ (mm)	n^{act}	$\max(\mathbf{F}^{act})$ (kN)	MIP-Gap	Mass savings
Adaptive	4766	4393	373	260	4	500	0%	38%
Passive	7641	7641	-	328	-	-	0%	

Figure 6 (a) GS 4x1, SR 5/1 (b) passive (c) adaptive

5. Conclusion

Force-parallel actuation has received little attention since it has been perceived as inherently constrained by the strain limits of the housing element. This work provides numerical evidence showing that in non-stiffness-governed problems, force-parallel actuators can effectively reduce the stress response in elements subjected to high forces. This in turn results in better quality element sizing distribution that can yield significant system mass savings compared to configuration using force-serial actuators.

In stiffness-governed scenarios, preliminary results show that, depending on the force capacity limit and other factors (e.g., initial ground structure and boundary conditions), the possibility to combine force-serial and force-parallel actuators yields configuration of minimum global system mass. In this scenario, force-serial actuators are placed on elements that take lower forces, e.g. upper-level columns and bracing in multi-story buildings, while force-parallel actuators are placed on critically loaded elements, e.g. lower-level columns and bracing.

Future work will consider other configurations and carry out a systematic parameter analysis to generalize the conclusions reached in this article.

Acknowledgments

References

[1] S. Utku, *Theory of adaptive structures: incorporating intelligence into engineered products*. CRC Press, 1998.

[2] A. M. Reinhorn, T. T. Soong, M. A. Riley, R. C. Lin, S. Aizawa, and M. Higashino, "Full-Scale Implementation of Active Control. II: Installation and Performance," *J. Struct. Eng.*, vol. 119, no. 6, pp. 1935–1960, Jun. 1993, doi: 10.1061/(ASCE)0733-9445(1993)119:6(1935).

[3] S. Korkmaz, "A review of active structural control: challenges for engineering informatics," *Comput. Struct.*, vol. 89, no. 23, pp. 2113–2132, Dec. 2011, doi: 10.1016/j.compstruc.2011.07.010.

[4] W. Sobek, "Ultra-lightweight construction," *Int. J. Space Struct.*, vol. 31, no. 1, pp. 74–80, Mar. 2016, doi: 10.1177/0266351116643246.

[5] A. P. Reksowardojo and G. Senatore, "Design of ultra-lightweight and energy-efficient civil structures through shape morphing," *Comput. Struct.*, vol. 289, p. 107149, Dec. 2023, doi: 10.1016/j.compstruc.2023.107149.

[6] D. Efinger, A. Ostertag, M. Dazer, D. Borschewski, S. Albrecht, and B. Bertsche, "Reliability as a Key Driver for a Sustainable Design of Adaptive Load-Bearing Structures," *Sustainability*, vol. 14, no. 2, Art. no. 2, Jan. 2022, doi: 10.3390/su14020895.

[7] G. Senatore, P. Duffour, and P. Winslow, "Energy and Cost Assessment of Adaptive Structures: Case Studies," *J. Struct. Eng.*, vol. 144, no. 8, p. 04018107, Aug. 2018, doi: 10.1061/(ASCE)ST.1943-541X.0002075.

[8] A. P. Reksowardojo, G. Senatore, M. Bischoff, and L. Blandini, "Design and Control Benchmark of Rib-Stiffened Concrete Slabs Equipped with an Adaptive Tensioning System," *J. Struct. Eng.*, vol. 150, no. 1, p. 04023200, Jan. 2024, doi: 10.1061/JSENDH.STENG-12320.

[9] M. Nitzlader, S. Steffen, M. J. Bosch, H. Binz, M. Kreimeyer, and L. Blandini, "Designing Actuation Concepts for Adaptive Slabs with Integrated Fluidic Actuators Using Influence Matrices," *CivilEng*, vol. 3, no. 3, Art. no. 3, Sep. 2022, doi: 10.3390/civileng3030047.

[10] A. P. Reksowardojo, G. Senatore, M. Bischoff, and L. Blandini, "Design and control of high-speed railway bridges equipped with an under-deck adaptive tensioning system," *J. Sound Vib.*, vol. 579, p. 118362, Jun. 2024, doi: 10.1016/j.jsv.2024.118362.

[11] G. Senatore and Y. Wang, "Topology Optimization of Adaptive Structures: New Limits of Material Economy," *Comput. Methods Appl. Mech. Eng.*, vol. 422, p. 116710, Mar. 2024, doi: 10.1016/j.cma.2023.116710.

[12] M. Böhm *et al.*, "Input modeling for active structural elements - extending the established FE-Work for modeling of adaptive structures," in *2020 IEEE/ASME International Conference on Advanced Intelligent Mechatronics (AIM)*, Jul. 2020, pp. 1595–1600. doi: 10.1109/AIM43001.2020.9158996.

[13] L. Blandini *et al.*, "D1244: Design and Construction of the First Adaptive High-Rise Experimental Building," *Front. Built Environ.*, vol. 8, 2022, Accessed: Jul. 01, 2022. [Online]. Available: https://www.frontiersin.org/article/10.3389/fbuil.2022.814911

[14] G. Senatore and A. P. Reksowardojo, "Force and Shape Control Strategies for Minimum Energy Adaptive Structures," *Front. Built Environ.*, vol. 6, p. 105, Jul. 2020, doi: 10.3389/fbuil.2020.00105.

[15] W. Dorn, R. Gomory, and H. J. Greenberg, "Automatic design of optimal structures," *Journal de mècanique*, vol. 3, no. 1, pp. 25–52, 1964.

[16] M. Cococcioni and L. Fiaschi, "The Big-M method with the numerical infinite M," *Optim. Lett.*, vol. 15, no. 7, pp. 2455–2468, Oct. 2021, doi: 10.1007/s11590-020-01644-6.

[17] van Halteren Technologies, "Electro Hydraulic Actuator," 2022. [Online]. Available: https://vanhalteren.com/application/files/2016/7948/1768/Datasheet_Electro_Hydraulic_Actuator.pdf

[18] Gurobi Optimization, LLC, "Gurobi Optimizer Reference Manual." 2023. [Online]. Available: https://www.gurobi.com